Hindawi Publishing Corporation
Journal of Nanomaterials
Volume 2013, Article ID 480164, 9 pages
http://dx.doi.org/10.1155/2013/480164

Research Article

Optical Characterization and Growth Mechanism of Combination of Zinc Oxide Nanowires and Nanorods at Various Substrate Temperatures

Poulami Ghosh and A. K. Sharma

Department of Physics, Indian Institute of Technology Guwahati, Guwahati 781039, Assam, India

Correspondence should be addressed to A. K. Sharma; aksharma@iitg.ernet.in

Received 21 April 2013; Revised 23 July 2013; Accepted 7 August 2013

Academic Editor: Gong Ru Lin

We report on the growth of ZnO nanostructures on *n*-type silicon substrate using pulsed laser deposition technique at substrate temperature ranging from room temperature to 600°C for one hour. We observe both rod- and wire-like structures with different dimensions at room temperature, 150°C, and 450°C substrate temperatures and only wire-like structures at 300°C and 600°C. These combinations of different shapes have been attributed to the initial growth of nanostructures (nucleation sites) on the surface obtained during the deposition for 20 minutes. The narrowing in the full-width-half-maximum of the peak corresponding to (002) plane of XRD is looked upon as another possible explanation. The blue shift of the peak at 396 nm observed in the photoluminescence is due to the quantum confinement. The intensity of E_2(high) mode at 437 cm^{-1} increases indicating improvement in crystallinity with the substrate temperature.

1. Introduction

Zinc oxide (ZnO) is one of the wide band gap semiconducting materials, because of its band gap of 3.37 eV at room temperature (RT), large exciton binding energy of about 60 meV, and distinguished surface effect (with up to 1.53 eV band bending) [1–3] it has attracted intensive research efforts for its versatile applications such as memory [4], transistors [5], light emission [6], gas sensing [7], antireflection [8], and UV photodetection [8, 9]. Despite some disadvantages like limited uniformity of films and growth of particulates, pulsed laser deposition (PLD) is a versatile technique for thin film deposition. ZnO nanostructures have been deposited on sapphire, silicon (Si), and glass substrates [10–13]. Several types of ZnO nanostructures including nanowires and nanorods, nanoparticles assisted nanowires have been reported by hydrothermal growth and pulsed laser deposition [14, 15].

ZnO has been grown in various shapes like nanorods, nanowires, nanobelts, and so forth, [16] under experimental conditions which have been conducive in the growth of only one specific kind of shape or structure, say, only nanorods or only nanowires. In this paper, we report on the growth of ZnO nanostructures that appear either as a combination of nanorods and nanowires or nanowires or nanorods alone. These structures have been grown using PLD technique on *n*-type silicon (Si) substrate at substrate temperature ranging from room temperature (RT) to 600°C. Both rod-like and a few wire-like structures have been observed at RT; both rod- and wire-like structures with different dimensions have been observed at 150°C and 450°C substrate temperature; and only wire-like structures have been observed at 300°C and 600°C. The structural and optical characterization of these nanostructures has been carried out using X-ray diffraction (XRD), field-emission scanning electron microscopy (FE-SEM), photoluminescence (PL) and Raman spectroscopy, respectively. The formation of only nanorods/wires or both the nanorods and nanowires was explained in terms of the surface morphology of nanoparticles grown for reduced deposition time (20 minutes).

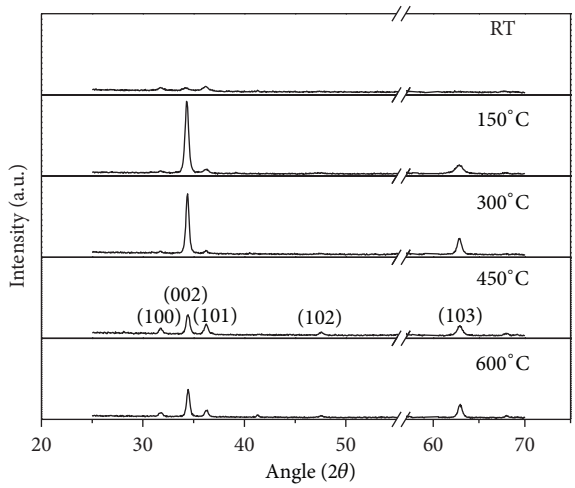

Figure 1: XRD spectra of ZnO thin films.

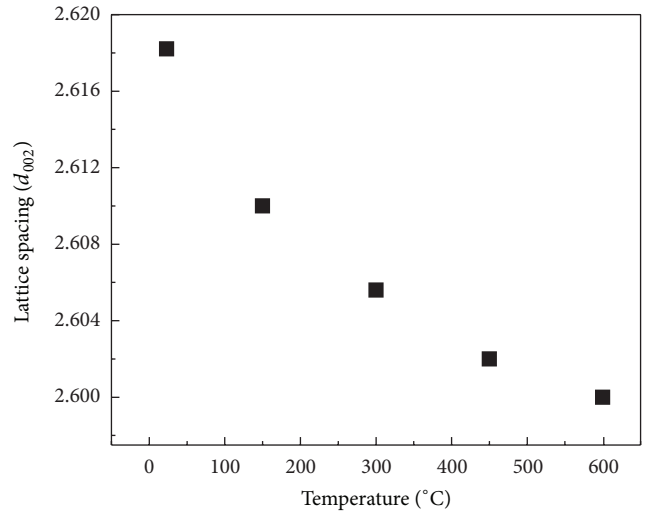

Figure 2: Lattice spacing of the ZnO thin films.

2. Material and Methods

ZnO targets were prepared using polyvinyl alcohol as a binder. The targets were pressed at 3 ton and sintered at 1000°C for 5 hours. The Q-switched Nd:YAG laser (Quanta laser, HYL-101) operated at a wavelength of 532 nm; pulse width (10 ns) with repetition rate of 10 Hz was focused on the surface of the ZnO target. The target was rotated continuously so that energy laser pulse falls on its fresh surface. The ZnO films were deposited on n-type silicon (Si) substrate at a base pressure of 10^{-5} mbar. The target-substrate distance was fixed at 4 cm. The deposition time was 20 and 60 minutes. The laser fluence was maintained at around 12 J/cm^2 during deposition. Oxygen (O_2) gas was used as the ambient gas. The films on Si(100) substrate were deposited at different substrate temperatures—RT (23°C), 150°C, 300°C, 450°C, and 600°C maintained at 0.1 mbar in the vacuum chamber.

We had deposited ZnO nanostructures for 20 minutes in order to understand only the growth mechanism of either only nanorods/wires or both nanorods and nanowires at the same deposition condition for 60 minutes growth.

3. Results and Discussions

3.1. XRD Analysis. XRD (seifert 3003-TT XRD) spectra of the nanostructures were recorded by using a CuKα1 source at a wavelength of 1.5406 Å. Figure 1 shows the XRD of the films deposited on n-type Si substrate at temperatures ranging from RT to 600°C with deposition time of 1 hour. Various peaks are identified within the literature [17]. The intensity of (002) peak corresponding to 34.4° angle is relatively high compared to other peaks and indicates that the nanostructures have the hexagonal (wurtzite) structure [18]. The lattice parameters of bulk ZnO and ZnO nanostructures grown at 300°C substrate temperature for (002) plane calculated from XRD data are a = 3.184 Å, c = 5.199 Å and a = 3.192 Å, c = 5.212 Å, respectively.

The difference in the lattice parameters in bulk ZnO and ZnO nanostructures indicates an increase in the local strain around the lattice defects. This strain is compressive between ZnO and Si [19]. The strain calculated for ZnO nanostructures deposited at different substrate temperatures using the relation [20]

$$T \tan\theta = \frac{\lambda}{D\cos\theta} - \beta, \quad (1)$$

where T is the lattice strain, 2θ is the location of the peak, λ is the X-ray radiation wavelength, D is the grain size, and β is the full-width-half-maximum (FWHM) corresponding to the peak, showed that the nanostructures have more strain at RT ($T = 3.76 \times 10^{-3}$) and are reduced at higher substrate temperatures ($T = 2.33 \times 10^{-3}$ at 600°C). The lattice spacing (d_{002}) of bulk ZnO is 2.603 Å [21]. Figure 2 shows the variation of the lattice spacing (d_{002}) with substrate temperature and observes that d_{002} at 300°C and 450°C is close to the bulk ZnO value indicating the strains in the nanostructures are low.

The nanostructures grown at 150°C and 300°C substrate temperatures are strongly c-axis oriented than that deposited at RT, 450°C, and 600°C. For the nanostructures deposited at RT and 600°C, the peak at 41.3° corresponds to zinc as shown in Figure 3 [22]. The presence of Zn indicates the deficiency of oxygen in the films. The fluence of the incident beam is beyond the ablation threshold. Thus, the interaction of laser with ZnO will also result in the production of Zn. Since there is no surface mobility at RT on the substrate, we expect some Zn on the film and hence its appearance in the XRD data. At high temperature (600°C), Zn will remain in the molten state. At other temperatures molten Zn from the plasma plume will readily combine with the surrounding oxygen to form ZnO.

The degree of crystal orientation is defined as $P = I(002)/\sum I(hkl)$, where $I(002)$ is the intensity of (002) diffraction peak and $\sum I(hkl)$ is the intensity of all diffraction peaks [23]. The variation of integrated intensity ratio $I(002)/I(101)$ and the FWHM of the (002) plane at 34.4° with the substrate temperature are shown in Figure 4. It shows that this ratio increases from RT to 300°C and then

Table 1: Full-width-half-maximum (from XRD) and size distribution of nanowires and nanorods at various substrate temperatures.

Substrate temperature (°C)	FWHM (002) (degree)	Nanowire diameter (nm)	Nanorod diameter (nm)
RT (23)	0.61	65	165
150	0.422	60	560
300	0.373	120	—
450	0.423	80	420
600	0.374	78	—

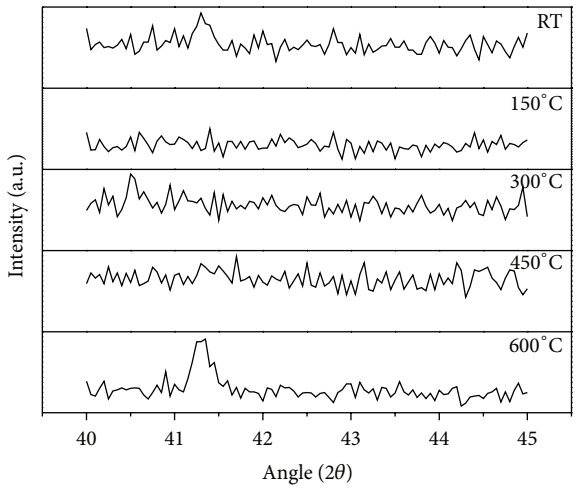

Figure 3: XRD spectra of ZnO thin films (from $2\theta = 40^{\circ}$ to 45°).

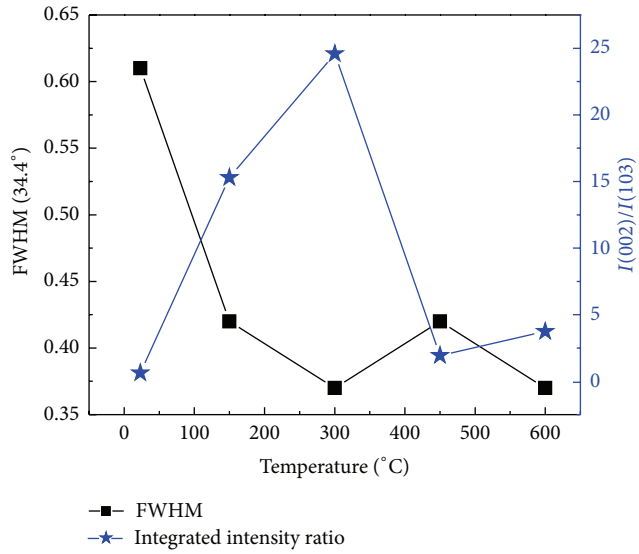

Figure 4: Variation of integrated Intensity ratio of (002) and (101) XRD plane and FWHM of (002) plane of ZnO with substrate temperature.

decreases gradually from 300°C to 600°C, indicating that the nanostructures grown at 150°C and 300°C, are highly oriented along (002) direction and more so at 300°C whereas no preferred orientation is observed for the nanostructures grown at other substrate temperatures. The FWHM is narrower for the nanostructures grown at 300°C and 600°C, whereas it is broader at RT and in between 150°C and 450°C. The narrower the FWHM the better the crystallinity. Other planes also showed similar behavior in FWHM.

3.2. Surface Morphology. The FE-SEM (Sigma, Zeiss, Oberkochen, Germany) images of the deposited nanostructures are shown in Figure 5. At RT, 150°C, and 450°C substrate temperatures both the rod- and wire-like nanostructures are observed, whereas at 300°C and 600°C only wire-like structures are observed. There are very few belt-like structures at RT. Such a distribution is attributed to the wide distribution of the size of nanoparticles deposited on the surface of the substrate that formed the nucleation sites for further growth of nanowires/rods/belts as observed in our recent work on the deposition of ZnO nanostructures for 20 minutes under the same experimental conditions, and the surface morphology of these nanostructures is shown in Figure 5. We observed the formation of diamond-like structures on the surface apart from other particulates at 150°C and 450°C substrate temperatures; however, very smooth surfaces with nanoparticles were observed at 300°C and 600°C, respectively. The particles in the range of a few tens of nanometer will result in the growth of nanowires, whereas those with larger size, a few hundreds of nanometers, will result in the growth of nanorods. Very likely, a few of the nucleation sites with smaller dimension will merge in a way so as to favour the growth of nanobelts (as observed at RT). Therefore, we believe that such surface morphologies have resulted in the growth of combination of rod- and wire-like or wire-like nanostructures. We have also attempted to understand this growth by looking at the variation in FWHM of the peaks corresponding to the planes (002), (101), and (103) as shown in Figure 7. The contribution to both the wire- and rod-like structures seems to be coming from the (101) and (103) planes which shows broader FWHM at 150°C and 450°C as compared to that for only wire-like structures in which case it is narrower at 300°C and 600°C. Figures 8(a)–8(h) show the distribution of the diameter of the grown nanowires/rods at different substrate temperatures (summarized in Table 1).

3.3. Photoluminescence. The PL spectra (ThermoSpectronic, AB2, monochromator xenon flash lamp) of ZnO nanostructures at different substrate temperatures are shown in Figure 9. The nanostructure deposited at RT has the near band edge peak at 396 nm, at 150°C and 450°C it is at 397 nm, at 300°C it is 389 nm, and at 600°C it is at around

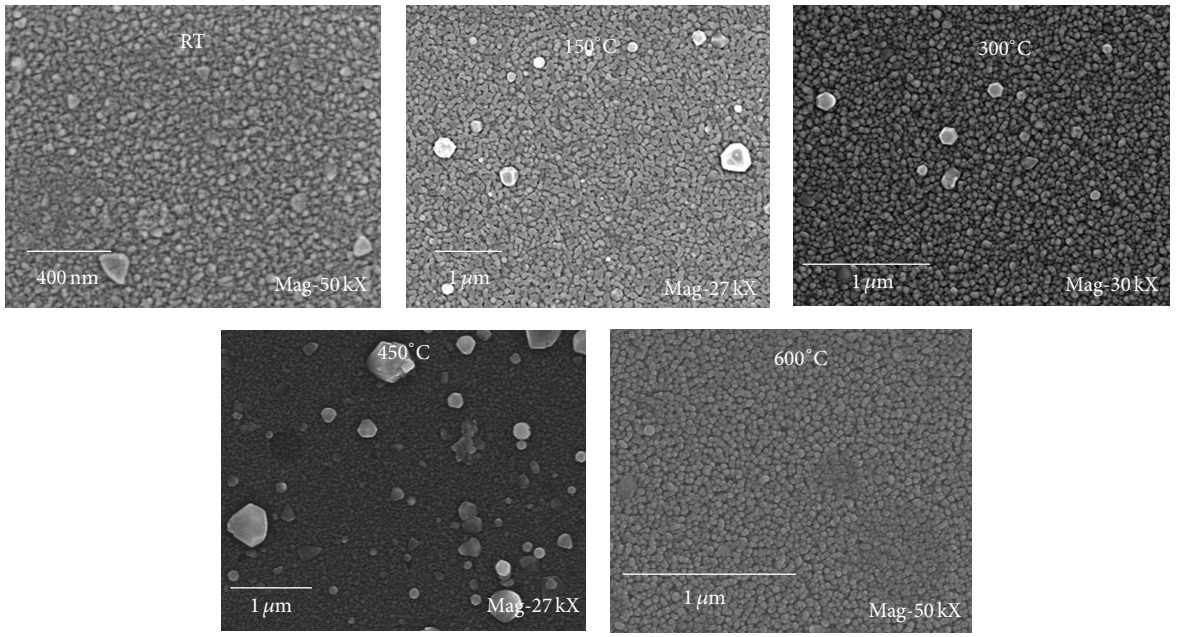

Figure 5: FE-SEM images of ZnO thin films deposited for 20 minutes.

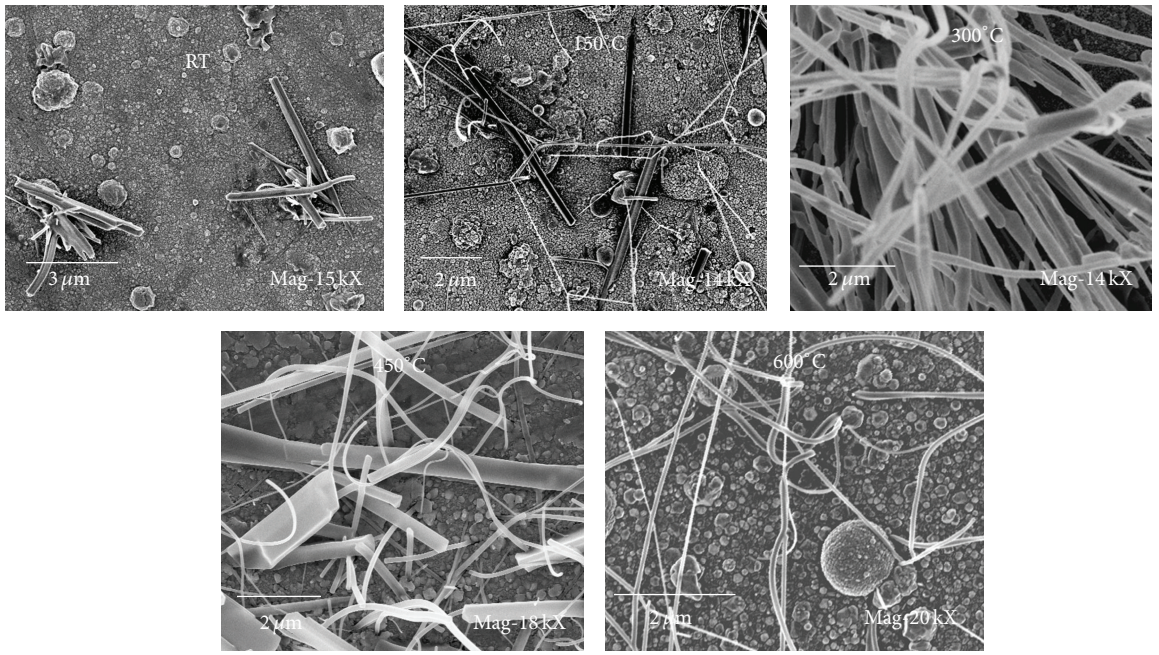

Figure 6: FE-SEM images of ZnO thin films deposited for 60 minutes.

398 nm. The blue shift in the PL of nanorods and nanowires has been attributed to the quantum confinement resulting from the decrease in the diameter of these structures [24–26]. In our case, we see that (Figure 6) the nanorods and nanowires combination at 150°C got converted to nanowires at 300°C, and accordingly the average size of the nanorods and nanowires combination at 150°C has reduced to around 120 nm at 300°C (Table 1). Again, we see that the combination of the nanorods and nanowires is observed in the FE-SEM images at 450°C and resulting in an increase in the average size. For the nanostructures deposited only at 600°C substrate temperature, a small peak is observed at 377 nm. This is due to the excitonic emission [11, 17, 27]. A small intense peak at the blue-green region is also observed at 467 nm for all nanostructures [28]. The 467 nm peak is related to the defect levels. The nanostructures grown at 300°C show a lower intense blue-green peak than the nanostructures grown at RT, 150°C, 450°C, and 600°C indicating less defects for

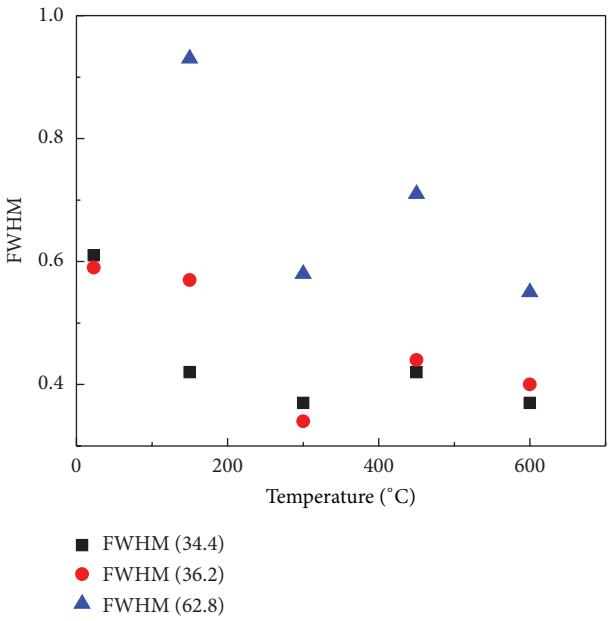

Figure 7: FWHM for the XRD peaks corresponding to (002), (101) and (103) planes of ZnO thin films.

the nanostructures grown at 300°C. Also, a broad peak in the red region is observed at around 595–600 nm [29] (Figure 10). It is clear that at substrate temperature of 450°C this peak is more prominent than the nanostructures deposited at other temperatures. This is due to the defect related states such as oxygen vacancy and zinc interstitials [28, 29]. The defects are minimum for the nanostructures grown at 300°C substrate temperature.

Figure 11 shows the variation of FWHM of UV-PL peak and the ratio of UV to defect level emission (blue-green emission) with substrate temperature and gives information about the structural defects [12]. The low intensity of deep level emission as compared to UV emission is the indication of low structural defect [30]. It is clear that the UV to blue-green PL ratio is maximum for the structures grown at 300°C indicating the low structural defect of the nanostructures. Also, among the grown nanostructures, the FWHM is narrowest at 300°C, indicating that the optical properties of the nanostructures are enhanced as we increase the substrate temperature up to 300°C, decrease by further increasing substrate temperature, and have better crystallinity [17, 21, 31].

The Gaussian fitting of the PL spectra of all the nanostructures is shown in the inset of Figure 9 at various substrate temperatures. The lists of the Gaussian-fitted PL peaks are given in Table 2.

3.4. Raman Analysis. The Raman spectra (Lab Ram HR-800, Jobin Yvon) were recorded by using an Argon ion laser operating at a wavelength of 488 nm. The frequencies of the fundamental optical modes in bulk ZnO and ZnO nanostructures are summarized in Table 3. Figure 12 shows the Raman spectra of the grown nanostructures, where E_1(TO), E_2(high), and A_1(LO) modes are observed. The E_2(high) peak is weak in intensity for the nanostructure deposited at RT, whereas the peak intensity increases continuously beyond RT till 600°C. The presence of E_2(high) peak confirms the wurtzite structure of ZnO [32] and suggests that all the nanostructures except the nanostructure grown at RT are wurtzite in nature, and it improves as the substrate temperature is increased. The E_2(high) peak is at 438 cm^{-1} for all the nanostructures, and this value matches with the E_2(high) peak of ZnO nanorods [17] as also evident from the FE-SEM images. E_1(TO) mode is prominent at low temperatures, that is, at RT and 150°C but with the increase in substrate temperature, the intensity of this mode diminishes and it vanishes at 600°C substrate temperature. A_1(LO) mode, on the other hand, is prominent at high temperatures, that is, at 450°C and 600°C, respectively. We attribute this dominance to the combination of wire- and rod-like structures (as observed in the FE-SEM analysis) and perhaps more contribution from the nanorods (see Table 3). A_1(LO) mode appears only when the *c*-axis of wurtzite ZnO is parallel to the sample surface [17]. The high intensity and narrowing of the E_2(high) peak at 450°C and 600°C substrate temperatures as compared to other peaks are due to the confinement (from rods to wires). However, in the case of nanostructure at 450°C substrate temperature, the presence of diamond-like structures might contribute to the enhancement of the peak intensity. The broad peaks at 334 cm^{-1} and 665 cm^{-1} for bulk ZnO are the second- and fourth-order overtones [33, 34], and they belong to the multiphonon process [35]. All ZnO nanostructures in the present work showed only one component of the multiphonon emission peak at 667 cm^{-1}. The shifting in E_1(TO) mode can be attributed to the stress in the film in contact with the substrate [36] as discussed in the XRD analysis. The Raman peak at 303 cm^{-1} is observed due to the multiphonon feature of silicon [37, 38].

Table 2: PL peaks obtained after Gaussian fit of the data at various substrate temperatures.

Substrate temperature (°C)	Location of PL peaks (nm)
RT (23)	392, 419,[a] 434, 458
150	397, 426,[b] 444, 467,[d] 484
300	389, 419,[a] 435, 467,[d] 489
450	395, 421,[a] 435, 456,[c] 602[c]
600	377, 402, 467[d]

[a]Due to interstitial oxygen [32], [b]due to the interstitial Zn [32], [c]due to oxygen vacancies [28], [d]blue-green emission [27].

4. Conclusion

The XRD results showed the strong *c*-axis orientation and the wurtzite nature of the ZnO nanostructures. Comparing the XRD and PL results, it is shown that the nanostructures grown at 300°C are well crystalline and have less defects with better optical properties. ZnO wire- and rod-like structures were deposited on Si substrate at room temperature, 150°C, and 450°C substrate temperatures, whereas only wire-like structures were deposited at 300°C and 600°C. This growth is

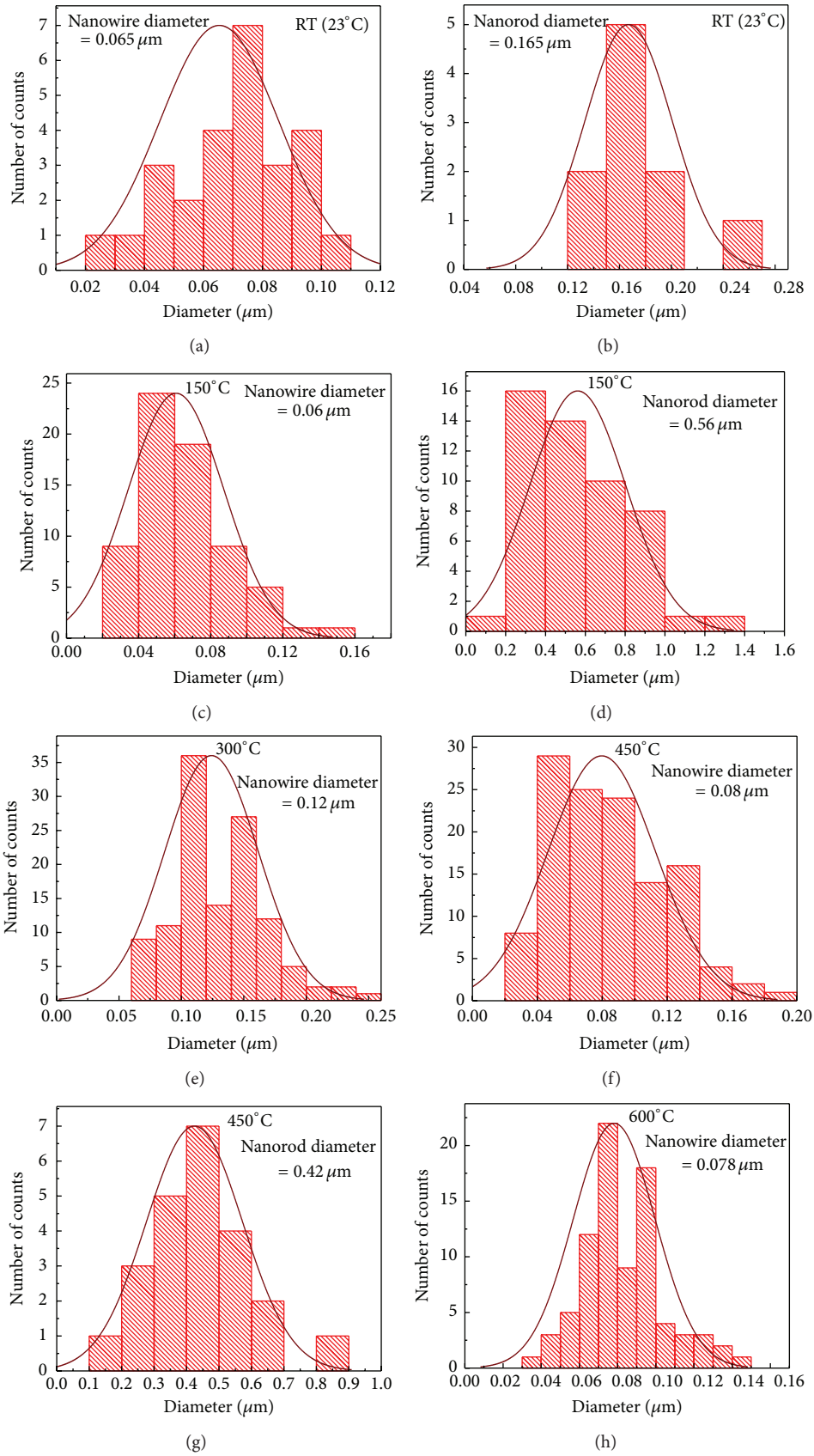

FIGURE 8: Diameter of nanorods/wires distribution of ZnO thin films deposited on Si substrate at 0.1 mbar O_2 pressure and at substrate temperature of ((a), (b)) RT, ((c), (d)) 150°C, (e) 300°C, ((f), (g)) 450°C, and (h) 600°C.

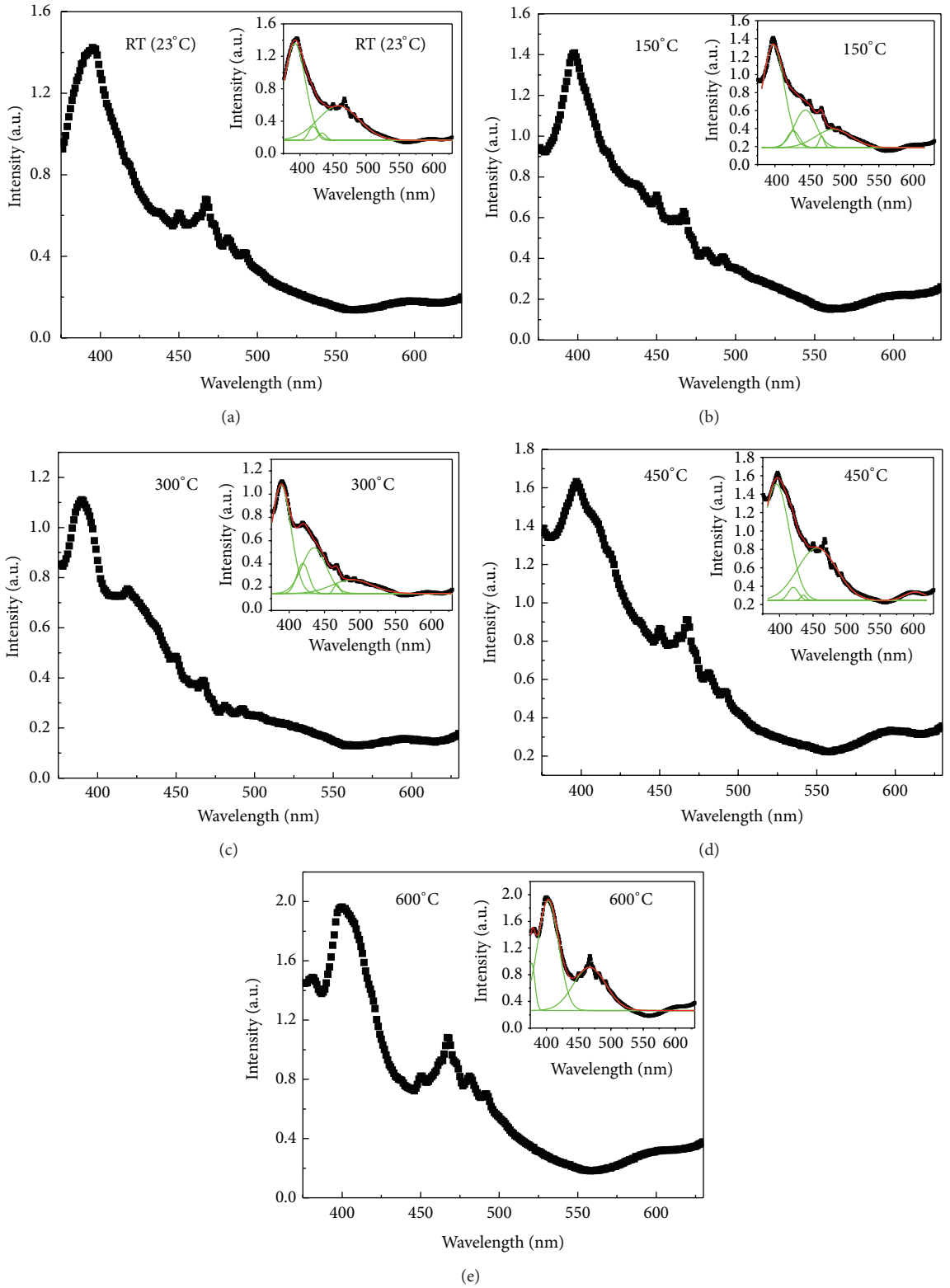

Figure 9: PL spectra of ZnO thin films in the range of 350–650 nm.

Table 3: Raman peaks at various substrate temperatures.

	E_2(low)	Multiphonon	A_1(TO)	E_1(TO)	E_2(high)	A_1(LO)	E_1(LO)
Bulk ZnO		334 cm^{-1}, 665 cm^{-1}	380 cm^{-1}	409 cm^{-1}	439 cm^{-1}		584 cm^{-1}
ZnO nanostructures [present work]		667 cm^{-1}		404 cm^{-1}	437 cm^{-1}	576 cm^{-1}	
ZnO nanorods [32]	101 cm^{-1}		380 cm^{-1}	407 cm^{-1}	437 cm^{-1}	574 cm^{-1}	583 cm^{-1}

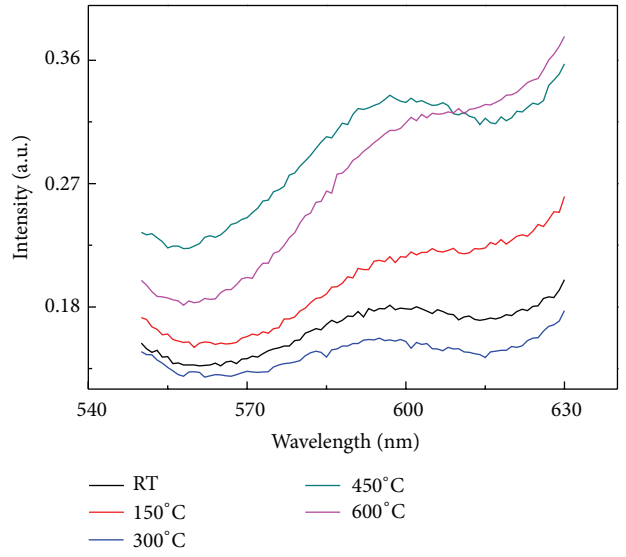

Figure 10: PL spectra of ZnO thin films in the range of 550–650 nm.

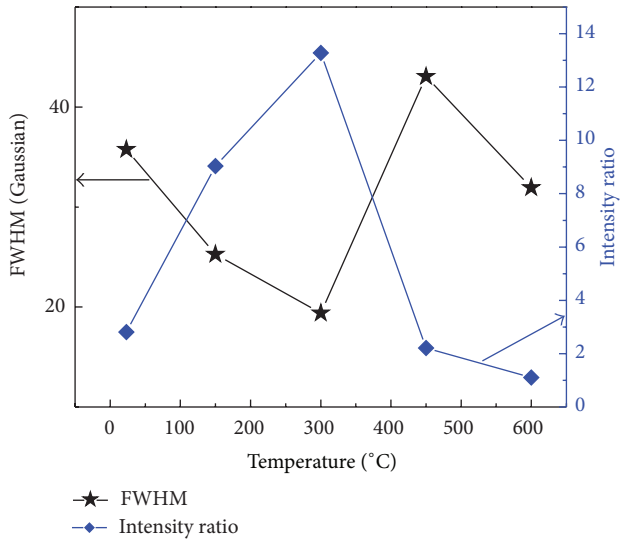

Figure 11: Intensity ratio of UV and visible emission of PL spectra and FWHM of UV emission with substrate temperature of ZnO thin films.

attributed to the wide range of size distribution of nanoparticles that acts as the nucleation site for the further growth indicating the importance of the deposition time in the initial growth of these structures. Possibly higher FWHM of (101) and (103) planes indicate that the growth of rod- and wire-like structures is favoured, whereas low FWHM indicates that growth of only wire-like structures is favoured.

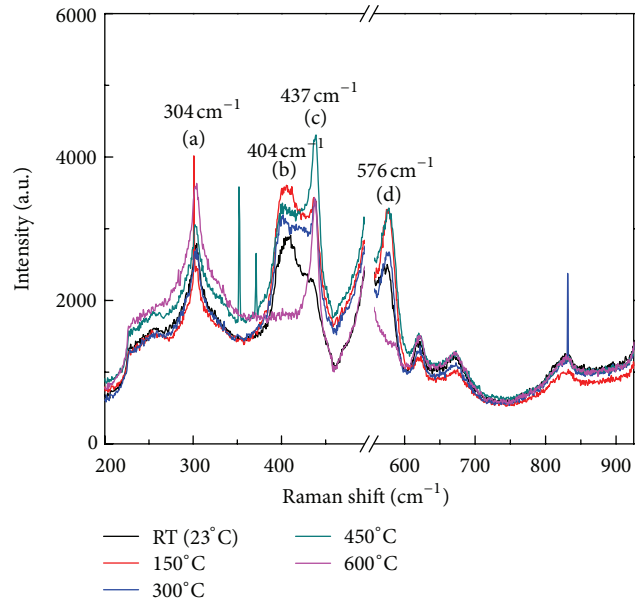

Figure 12: Raman spectra of ZnO thin films.

Acknowledgments

One of the authors (Poulami Ghosh) would like to thank the Council of Scientific and Industrial Research (CSIR), India, for the financial support and CIF, IIT Guwahati for research facilities.

References

[1] K. P. Jayadevan and T. Y. Tseng, "One-dimensional ZnO nanostructures," *Journal of Nanoscience and Nanotechnology*, vol. 12, no. 6, pp. 4409–4457, 2012.

[2] C.-Y. Chen, J. R. D. Retamal, I.-W Wu et al., "Probing surface band bending of surface-engineered metal oxide nanowires," *ACS Nano*, vol. 6, no. 11, pp. 9366–9372, 2012.

[3] C.-Y. Chen, M.-W. Chen, J.-J. Ke, C.-A. Lin, J. R. D. Retamal, and J.-H. He, "Surface effects on optical and electrical properties of ZnO nanostructures," *Pure and Applied Chemistry*, vol. 82, no. 11, pp. 2055–2073, 2010.

[4] Y.-D. Chiang, W.-Y. Chang, C.-Y. Ho et al., "Single-ZnO-nanowire memory," *IEEE Transactions on Electron Devices*, vol. 58, no. 6, pp. 1735–1740, 2011.

[5] D. Wang, H. W. Seo, C.-C. Tin et al., "Effects of postgrowth annealing treatment on the photoluminescence of zinc oxide nanorods," *Journal of Applied Physics*, vol. 99, no. 11, Article ID 113509, 2006.

[6] C.-Y. Chen, C.-A. Lin, M.-J. Chen, G.-R. Lin, and J.-H. He, "ZnO/Al_2O_3 core-shell nanorod arrays: growth, structural

characterization, and luminescent properties," *Nanotechnology*, vol. 20, Article ID 185605, 2009.

[7] J.-H. He, C.-H. Ho, and C.-Y. Chen, "Polymer functionalized ZnO nanobelts as oxygen sensors with a significant response enhancement," *Nanotechnology*, vol. 20, Article ID 065503, 2009.

[8] D.-S. Tsai, C.-A. Lin, W.-C. Lien, H.-C. Chang, Y.-L. Wang, and J.-H. He, "Ultra-high-responsivity broadband detection of Si metal-semiconductor-metal schottky photodetectors improved by ZnO nanorod arrays," *ACS Nano*, vol. 5, no. 10, pp. 7748–7753, 2011.

[9] M.-W. Chen, C.-Y. Chen, D.-H. Lien, Y. Ding, and J.-H. He, "Photoconductive enhancement of single ZnO nanowire through localized Schottky effects," *Optics Express*, vol. 18, no. 14, pp. 14836–14841, 2010.

[10] C. C. Wu, D. S. Wuu, P. R. Lin, T. N. Chen, and R. H. Horng, "Effects of growth conditions on structural properties of ZnO nanostructures on sapphire substrate by metal-organic chemical vapor deposition," *Nanoscale Research Letters*, vol. 4, no. 4, pp. 377–384, 2009.

[11] Ye. Sun, G. M. Fuge, and M. N. R. Ashfold, "Growth of aligned ZnO nanorod arrays by catalyst-free pulsed laser deposition methods," *Chemical Physics Letters*, vol. 396, no. 1–3, pp. 21–26, 2004.

[12] S. S. Kim and B.-T. Lee, "Effects of oxygen pressure on the growth of pulsed laser deposited ZnO films on Si(0 0 1)," *Thin Solid Films*, vol. 446, no. 2, pp. 307–312, 2004.

[13] L. Zhao, J. Lian, Y. Liu, and Q. Jiang, "Structural and optical properties of ZnO thin films deposited on quartz glass by pulsed laser deposition," *Applied Surface Science*, vol. 252, no. 24, pp. 8451–8455, 2006.

[14] S. Baruah and J. Dutta, "Hydrothermal growth of ZnO nanostructures," *Science and Technology of Advanced Materials*, vol. 10, Article ID 013001, 2009.

[15] R. Q. Guo, J. Nishimura, M. Matsumoto, D. Nakamura, and T. Okada, "Catalyst-free synthesis of vertically-aligned ZnO nanowires by nanoparticle-assisted pulsed laser deposition," *Applied Physics A*, vol. 93, no. 4, pp. 843–847, 2008.

[16] Z. L. Wang, "ZnO nanowire and nanobelt platform for nanotechnology," *Materials Science and Engineering R*, vol. 64, no. 3-4, pp. 33–71, 2009.

[17] R. Zhang, P. G. Yin, N. Wang, and L. Gou, "Photoluminescence and Raman scattering of ZnO nanorods," *Solid State Sciences*, vol. 11, no. 4, pp. 865–869, 2009.

[18] P. S. Kumar, A. D. Raj, D. Mangalaraj, and D. Nataraj, "Growth and characterization of ZnO nanostructured thin films by a two step chemical method," *Applied Surface Science*, vol. 255, no. 5, pp. 2382–2387, 2008.

[19] X. M. Teng, H. T. Fan, S. S. Pan, C. Ye, and G. H. Li, "Photoluminescence of ZnO thin films on Si substrate with and without ITO buffer layer," *Journal of Physics D*, vol. 39, p. 471, 2006.

[20] B. D. Cullity, *Elements of X-Ray Diffraction*, Addison-Wesley, Reading, Mass, USA, 1978.

[21] J. Zhao, L. Hu, Z. Wang, J. Sun, and Z. Wang, "ZnO thin films on Si(1 1 1) grown by pulsed laser deposition from metallic Zn target," *Applied Surface Science*, vol. 253, no. 2, pp. 841–845, 2006.

[22] S. Cho, J. Ma, Y. Kim, Yi. Sun, G. K. L. Wong, and J. B. Ketterson, "Photoluminescence and ultraviolet lasing of polycrystalline ZnO thin films prepared by the oxidation of the metallic Zn," *Applied Physics Letters*, vol. 75, p. 2761, 1999.

[23] A. Mohanto and R. K. Thereja, "Photoluminescence study of ZnO nanowires grown by thermal evaporation on pulsed laser deposited ZnO buffer layer," *Journal of Applied Physics*, vol. 104, Article ID 044906, 2008.

[24] X. Mu, I. B. Zotova, Y. J. Ding, H. Yang, and G. J. Salamo, "Observation of an anomalously large blueshift of the photoluminescence peak and evidence of band-gap renormalization in InP/InAs/InP quantum wires," *Applied Physics Letters*, vol. 79, p. 1091, 2001.

[25] C.-W. Chen, K.-H. Chen, C.-H. Shen, J.-J. Wu, H.-I. Wen, and W.-F. Pong, "Anomalous blueshift in emission spectra of ZnO nanorods with sizes beyond quantum confinement regime," *Applied Physics Letters*, vol. 88, Article ID 241905, 2006.

[26] Y. Yan, Z.-M. Liao, Y.-Q. Bie et al., "Luminescence blue-shift of CdSe nanowires beyond the quantum confinement regime," *Applied Physics Letters*, vol. 99, Article ID 103103, 2011.

[27] S. Chakraborty and P. Kumbhakar, "Observation of exciton-phonon coupling and enhanced photoluminescence emission in ZnO nanotwins synthesized by a simple wet chemical approach," *Materials Letters*, vol. 100, pp. 40–43, 2013.

[28] Y. H. Yang, Y. Feng, and G. W. Yang, "Experimental evidence and physical understanding of ZnO vapor-liquid-solid nanowire growth," *Applied Physics A*, vol. 102, no. 2, pp. 319–323, 2011.

[29] J. Dai, C. X. Xu, Z. L. Shi et al., "Three-photon absorption induced whispering gallery mode lasing in ZnO twin-rods microstructure," *Optical Materials*, vol. 33, no. 3, pp. 288–291, 2011.

[30] S. Y. Hu, Y. C. Lee, J. W. Lee, J. C. Haung, J. L. Shen, and W. Water, "The structural and optical properties of ZnO/Si thin films by RTA treatments," *Applied Surface Science*, vol. 254, no. 6, pp. 1578–1582, 2008.

[31] R. S. Ajimsha, R. Manoj, P. M. Aneesh, and M. K. Jayaraj, "Violet luminescence from ZnO nanorods grown by room temperature pulsed laser deposition," *Current Applied Physics*, vol. 10, no. 2, pp. 693–697, 2010.

[32] S. K. Panda and C. Jacob, "Surface enhanced Raman scattering and photoluminescence properties of catalytic grown ZnO nanostructures," *Applied Physics A*, vol. 96, no. 4, pp. 805–811, 2009.

[33] S. Chen, Y. Liu, C. Shao et al., "Structural and optical properties of uniform ZnO nanosheets," *Advanced Materials*, vol. 17, no. 5, pp. 586–590, 2005.

[34] S.-S. Wu, Q.-M. Jia, Y.-L. Sun, S.-Y. Shan, L.-H. Jiang, and Y.-M. Wang, "Microwave-hydrothermal preparation of flower-like ZnO microstructure and its photocatalytic activity," *Transactions of Nonferrous Metals Society of China*, vol. 22, no. 10, pp. 2465–2470, 2012.

[35] T. C. Damen, S. P. S. Porto, and B. Tell, "Raman effect in zinc oxide," *Physical Review*, vol. 142, no. 2, pp. 570–574, 1966.

[36] S. B. Yahia, L. Znaidi, A. Kanaev, and J. P. Petitet, "Raman study of oriented ZnO thin films deposited by sol-gel method," *Spectrochimica Acta A*, vol. 71, no. 4, pp. 1234–1238, 2008.

[37] S. Youssef, P. Combette, J. Podlecki, R. Al Asmar, and A. Foucaran, "Structural and optical characterization of ZnO thin films deposited by reactive RF magnetron sputtering," *Crystal Growth and Design*, vol. 9, no. 2, pp. 1088–1094, 2009.

[38] K. Wu, Q. Fang, W. Wang, M. A. Thomas, and J. Cui, "On the origin of an additional Raman mode at 275 cm^{-1} in N-doped ZnO thin films," *Journal of Applied Physics*, vol. 111, Article ID 063530, 2012.